Journal Homepage: http://ijcpe.uobaghdad.edu.iq
Iraqi Journal of Chemical and Petroleum Engineering
Vol. 27 No. 1 (March 2026) 1 – 12
EISSN: 2618-0707, PISSN: 1997-4884

Glutaraldehyde-crosslinked chitosan reinforced with nanoparticles for wastewater treatment: Chemical structure modification

Arwa Raad Ibrahim [a], Basma A. Abdul Majeed [a, *], Sanaa A. Al-Sahib [b]

a Department of Chemical Engineering, College of Engineering, University of Baghdad, Baghdad, Iraq
b Department of Chemistry, College of Science for Women, University of Baghdad, Baghdad, Iraq

Abstract

Lead (II) pollution from the various industries is a serious environmental problem that requires urgent attention due to its stability and non-biodegradability. Current research addresses the development of a natural polymer's chemical structure to produce an absorbent nanocomposite for lead removal. This development relied on the available functional groups (amino-NH_2 and hydroxyl-OH groups) in biopolymers to create adsorbent material through two steps. The first step was chemical bonding of chitosan with glutaraldehyde as a crosslinking agent (CT-GLA) using emulsion cross linking technique, followed by another bonding with a heterogeneous organic compound to provide additional functional groups (CT-GLA-PD). The second step involved supporting the compound with copper oxide nanoparticles (CT-GLA-PD-Cu) to improve characterizations of the adsorbent. The chemical structure of the materials prepared by paraffin dispersion followed by nanoparticle support was carried out in the current study to explain the functional groups that disappeared and formed during the preparation stages. The surface characterization and chemical composition of the adsorbent resulting from the two stages were performed using advanced descriptive techniques such as Fourier Transform Infrared spectroscopy, X-ray Diffraction, Field Emission Scanning Electron Microscope and Energy Dispersive X-ray. According to the experimental data, the chemical modification showed a significant enhancement in morphology properties and composition elements, which positively impacted removal efficiency. This structure development has been reflected in the lead removal efficiency compared to the raw adsorbent. The results showed that the adsorbent produced in the first stage achieved acceptable lead removal efficiency. This performance was further doubled after the use of nanoparticles as supporting material in the second stage.

Keywords: DBT oxidation; Adsorption; Chitosan; Copper oxide; Composite; Emulsion; Glutaraldehyde.

Received on 25/11/2025, Received in Revised Form on 03/01/2026, Accepted on 03/01/2026, Published on 30/03/2026

https://doi.org/10.31699/IJCPE.2026.1.1

1- Introduction

Industrial activities are among the most prominent sources of water pollution with heavy metals due to the intensity of chemical processes and inadequately treated outputs. Among these activities, oil industries are major source of pollution. These industries are the lifeblood of the modern economy, providing the world with the energy and raw materials necessary for manufacturing. However, this enormous advantage is balanced by serious environmental risks, from extraction through refining and processing to final consumption [1]. The real problem lies in the complexity of the materials produced during drilling and refining processes, and the accompanying release of harmful waste into the air, water, and soil. Contaminated water from various discharges from oil industries is one of the most significant challenges facing ecosystems. Therefore, understanding the nature of these pollutants and their sources is the key step towards creating a sustainable living environment. Heavy metals, including lead (II), are among these dangerous pollutants because of their ability to bioaccumulate in living and non-living environments. They are therefore an environmental threat to areas surrounding industrial and extractive operations, oil refineries, and oil drilling [2]. Previous field data have indicated that lead (II) contamination levels in wastewater from oil and gas drilling have reached 47 mg/L, which is dozens of times higher than environmentally acceptable values [3]. A similar study also reported that lead (II) was present at unacceptable levels in wastewater produced from oil refineries [4]. This issue may not be limited to the oil industry, but may also include other industries, as in a previous study conducted in southern of Iraq. They indicated that lead contamination levels in wastewater reached more than 9 mg per liter, while in sediments, it reached 30 mg per gram. According to international organizations, such as US Environmental Protection Agency, permissible levels of lead in wastewater do not exceed 0.1 mg/L, while the World Health Organization has suggested that permissible levels of this contaminant do not exceed 0.01 mg/L. Therefore, the presence of ecosystems at levels higher than the permissible level

*Corresponding Author: Email: basma-bdulmajeed@coeng.uobaghdad.edu.iq

requires significant treatment efforts [5]. Lead (II) takes different forms depending on the pH of the environment. Leaching of this ion into soil contributes to changes in its chemical composition. Furthermore, its ability to bioaccumulate in microorganisms and plants disrupts natural nutrient cycles [6]. These concerns have been seriously addressed by environmental experts through effective lead removal technologies and processes.

Lead removal from wastewater involves several techniques, including chemical precipitation supported by UF and MF filtration [7]. Ion exchange is another common method for removing lead, employing resins that capture lead ions [8]. Membrane techniques can also be used for lead removal [9]. However, adsorption approach is the most prominent technique due to its low cost and acceptable efficiency [10, 11]. Among these technologies are nanocomposites, due to their unique and distinct properties compared to other conventional methods. The current study proposed the use of chitosan as a raw biomaterial for subsequent development stages to create a nanocomposite adsorbent for lead removal from contaminated water. The choice of chitosan was based on its unique properties, including biodegradability, eco-friendly resource, and non-toxicity [12, 13]. Perhaps most importantly, it possesses functional groups (such as NH_2 and OH) that can be exploited in the development stages [14]. However, the chemical instability of chitosan in acidic conditions of contaminated water hinders its use as an effective adsorbent. Therefore, this development targets the poor mechanical properties of chitosan as well as improving the adsorption efficiency. The first step is modification by using glutaraldehyde, which is an organic compound and demonstrates significant effectiveness in many industrial and pharmaceutical applications as well as protein immobilization [15-20]. The current research proposes using this compound as a crosslinking agent between the polymer's chains. This crosslinking improves the physical and chemical properties of the natural polymer. However, this crosslinking may reduce the availability of the polymer's functional groups. Therefore, heterogeneous organic compound was also used to provide compensatory functional groups, while the copper oxide nanoparticles were linked as supporting. Furthermore, the research also suggested, as part of the improvement procedures for chitosan, the exploitation of the unique properties of copper nanoparticles.

2- Experimental work

2.1. Preparation

A 6% (w/v) chitosan solution (Pure chitosan, Thomas Baker company, India) was prepared using glacial acetic acid (99.9%, SRL, Sisco Research Laboratories PVT, Ltd) with continuous stirring via a magnetic stirrer at 25 °C. It was then emulsified in a medium consisting of 80 ml paraffin oil (Paraffin Liquid Light, SRL, Sisco Research Laboratories Pvt, Ltd) supplemented with ratio 4 ml of the emulsifying agent Span-80 (Sorbitan Monooleate, SRL, Sisco Research Laboratories Pvt, Ltd) while stirring [21]. Ten milliliters of glutaraldehyde solution (SDFCL) were added as a crosslinking agent to enhance polymer stability. The pH gradually adjusted from 2 to 9 until crosslinking was complete. The mixture was washed with petroleum ether and acetone solvents as well as distilled water, then dried in an oven at 60°C for 24 hours. The reflux system was prepared and set at 50°C for the second stage.

Chitosan-glutaraldehyde composite (CT-GLA) was added to react with Pyromellitic dianhydride (PMDA) in the dimethylformamide (DMF) solvent for 4.5 hours under continuous stirring. The product (CT-GLA-PD) was then filtered and washed with 0.1 mol/liter DMF, then with deionized water until the pH was adjusted to 7. In the second stage for production (CT-GLA-PD-Cu), 0.2 g of copper oxide was weighed and placed in 20 ml of tetrahydrofuran solvent, then sonicated for 60 min. Next, 100 mg of CT-GLA-PD was added under a refluxing system for four hours to followed by a drying system.

Fig. 1 shows simplified flow diagram of nanocomposite preparation. The development of the adsorption efficiency of the material prepared in this study was investigated by adsorption of lead from contaminated water. The stock solution used in the experiments was based on samples of wastewater from the washing of liquefied gas tanks. The simulated contaminated water was prepared with a concentration close to that recorded in the actual contaminated water. This was achieved by diluting of a lead nitrate solution prepared by a German company. The lead concentration was then measured using an atomic absorption spectrometer.

2.2. Characterization

The Characterizations stage involved analyzing the chemical structure of CT-GLA-PD and CT-GLA-PD-Cu using FTIR. XRD study examined how X-rays diffract from the atomic planes of nanoparticles to determine their crystalline structure. The morphology and surface features were analyzed by Field-Emission-Scanning-Electron-Microscopy (FESEM). In contrast, Energy Dispersive X-ray (EDX) was used to characterize the elemental composition of the nanocomposites.

3- Results and discussion

3.1. Chemical structure of CT-GLA-PD-Cu

Two modifications were made in the preparation processes: first, optimizing the amount of natural polymer (Ct) in preparation of CT-GLA, and second, incorporating copper-oxide nanoparticles into the final product (CT-GLA-PD) to improve its adsorption performance. Fig. 2 illustrates the mechanism of chemical cross-linking between chitosan chains through the glutaraldehyde organic compound. The amine group on the chitosan ring ($–NH_2$) attacks the carbonyl carbon of the aldehyde in the glutaraldehyde. These attacks lead to form a temporary C–N bond and creating an intermediate compound known as carbinolamine, while the remaining –CHO group is

free at the other end of the glutaraldehyde group. The glutaraldehyde molecule contains two aldehyde groups; therefore, a single molecule can react with two amines from two different chitosan chains to create a double bond between a carbon and a nitrogen atom as shown in Fig. 3. The presence of the absorption peak in the FTIR spectrum at 1641 cm^{-1} is structural evidence of the presence Schiff bases through the functional group (C=N). The reaction of the second end of the glutaraldehyde chain with second chitosan is responsible for the formation of crosslinks between the chitosan chains (a three-dimensional network) which improves the physical and chemical properties of the adsorbent, for example, reducing the solubility of the material and increasing its rigidity and thermal resistance.

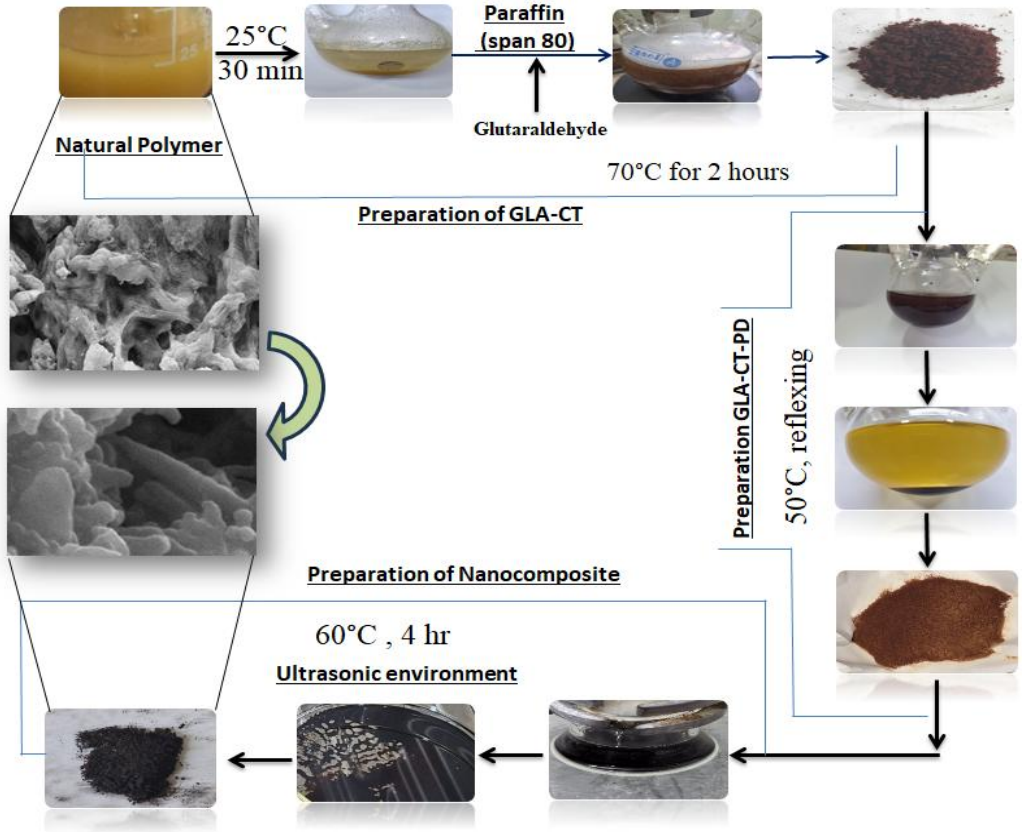

Fig. 1. A simplified flow diagram of nanocomposite preparation

This reaction requires mildly alkaline operating conditions to minimize the effect of amine ionization. Therefore, during the preparation, the pH gradually adjusted to alkaline until crosslinking was complete.

In another hand, OU and BO [22] indicated that the cross-linking of chitosan and Glutaraldehyde produces two water molecules. The presence of these molecules, in addition to the water used in the preparation of sodium hydroxide (added to adjust the pH during preparation), may lead to the formation of pyromellitic acid with the subsequently added Pyromellitic dianhydride. The process occurs through the hydrolysis of Pyromellitic dianhydride, causing the water molecules to break the anhydride bonds as shown in Fig. 4. This reaction results in the loss of the pyromellitic dianhydride's effectiveness with the CT-GLA compound. Therefore, a drying stage to remove any moisture from the CT-GLA before handling the Pyromellitic dianhydride in the next stage may be necessary to achieve chemical bonding efficiency.

The optimal bond between pyromellitic dianhydride and chitosan occurs via amines in the chitosan chain, leading to breaking one of the PMDA anhydride rings. This breakage forms crosslinking of two chitosan molecule chains to produce carboxyl functional group, followed by the breakage of the second ring from the opposite side of the PMDA itself, forming another carboxyl functional group. Kavianinia [23] reported that the association of pyromellitic dianhydride with chitosan occurs through amines forming an intermediate amic acid group as a cross-linking process between natural polymers.

However, in the current study, due to the prior association of the chitosan amino group with glutaraldehyde, the favored reaction of pyromellitic dianhydride is with the chitosan hydroxyl group, resulting in the opening of the two rings and the formation of carboxyl functional groups. In pyromellitic dianhydride, the first anhydride group attacks the hydrogen atom in the hydroxyl group (OH) in the chitosan molecule chains, breaking this anhydride ring and forming an ester bond that creates a carboxyl functional group. With a second hydroxyl group available in another chitosan chain, the breaking of the second anhydride ring is repeated, also forming another carboxyl functional group, as shown in Fig. 5.

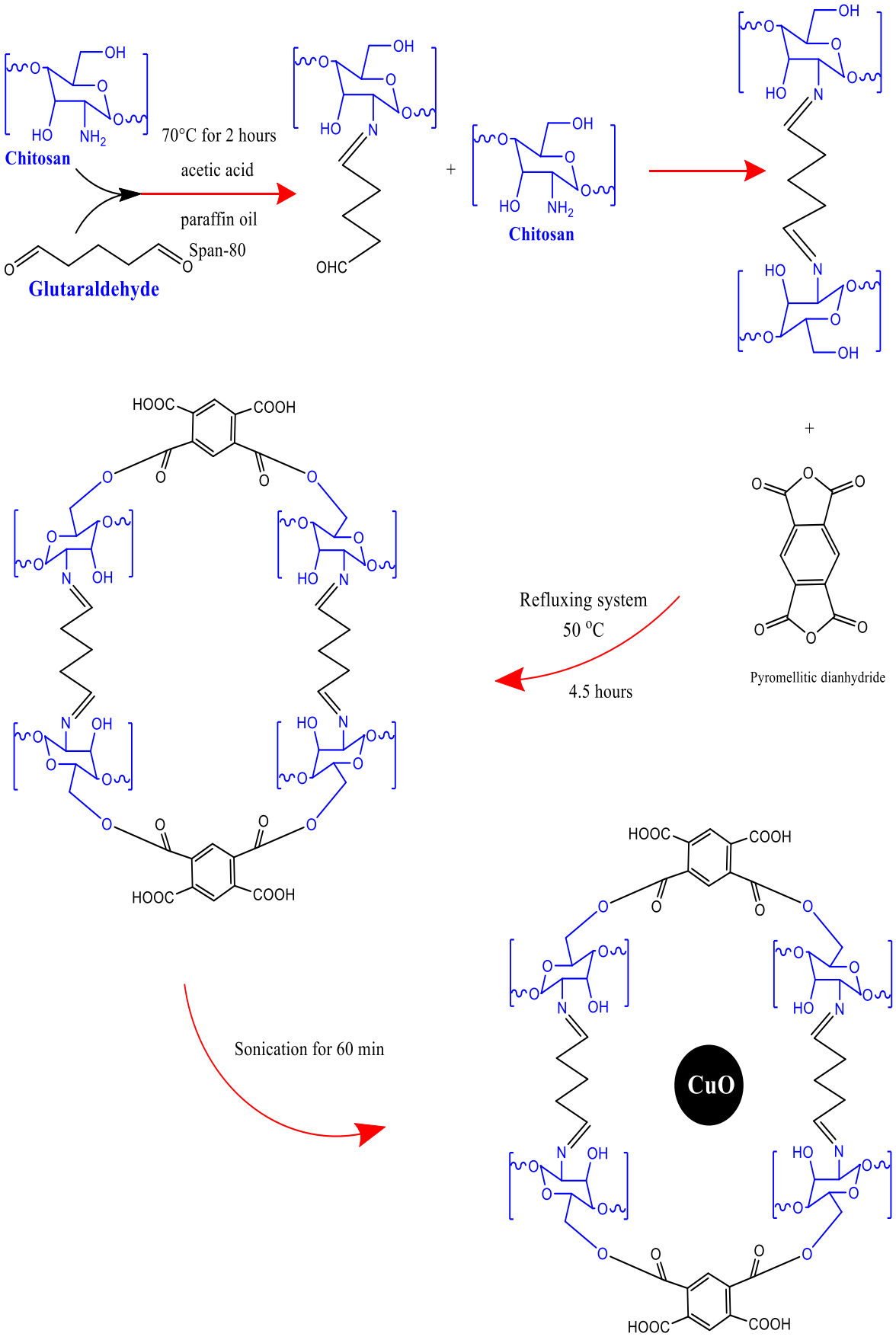

Fig. 2. Schematic diagram presenting the reaction mechanism of chitosan-glutaraldehyde and chitosan-glutaraldehyde-pyromellitic dianhydride

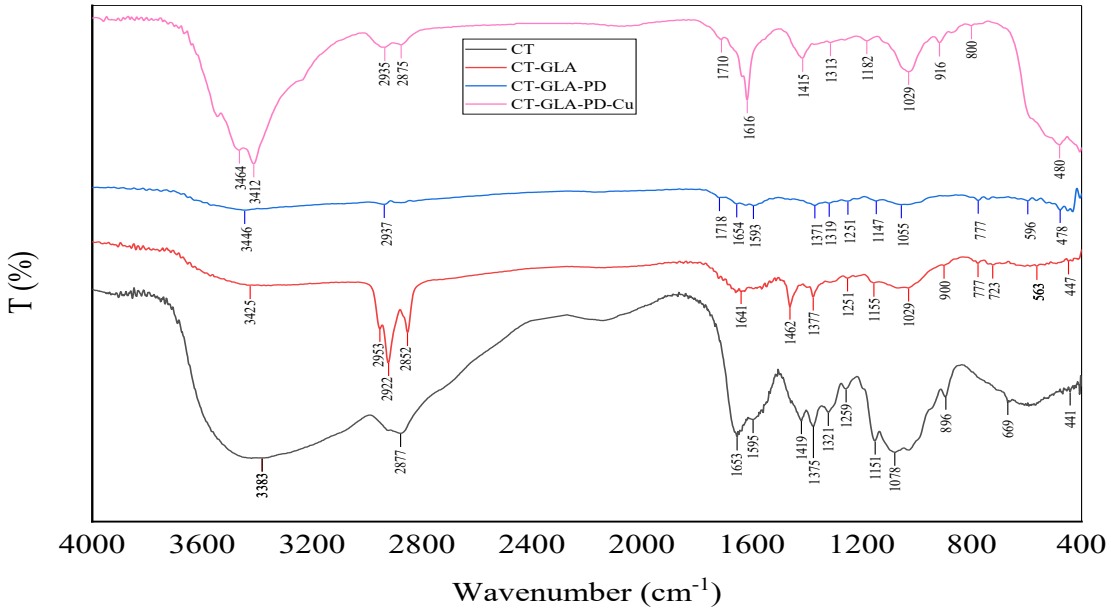

Fig. 3. FITR spectra of chitosan (CT), chitosan-glutaraldehyde (CT-GLA), chitosan-glutaraldehyde-pyromellitic dianhydride (CT-GLA-PD), chitosan-glutaraldehyde-pyromellitic dianhydride-copper (CT-GLA-PD-Cu)

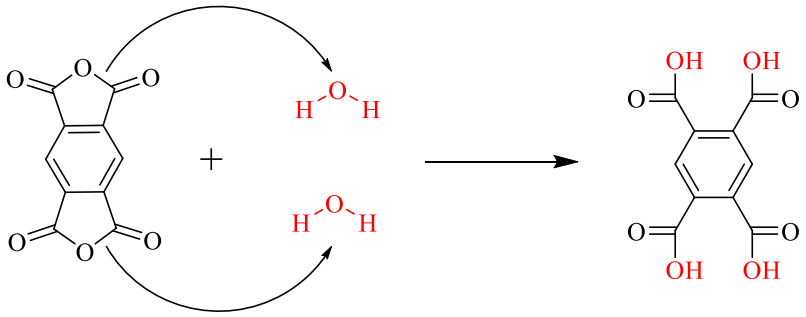

pyromellitic dianhydride water pyromellitic acid

Fig. 4. Schematic diagram presenting the reaction mechanism of chitosan and water

In the third stage of preparation, copper oxide nanoparticles were bonded under dispersive environmental conditions using ultrasound to inhibit particle agglomeration. This crosslinking process aimed to exploit the nanoscale properties of copper oxide to enhance and develop the chitosan material-based glutaraldehyde and Pyromellitic dianhydride. The structural bonding between copper particles and unenhanced chitosan occurs via primary amines and hydroxyl groups within coordination bonds [24]. In this study, due to the limited number of amine groups, the bonding will be via the hydroxyl group available in chitosan to form the core (copper oxide nanoparticles) and shell (modified chitosan chains) structure.

3.2. X-ray diffraction spectra

The X-ray diffraction Spectra patterns of the CT-GLA-PD and CT-GLA-PD-Cu NPs samples are shown in Fig. 6. The XRD pattern of the CT-GLA-PD and CT-GLA-PD-Cu NPs exhibits numerous clear peaks and a low background, confirming the well-crystallinity of the samples. XRD detected no impurities. In addition to the CT-GLA-PD-Cu peaks, the samples with CuO content clearly show the presence of CuO peaks at 2θ ~ 32.5, 35.5, 38.7, 48.8, 53.5, 58.17, 61.5, 66.2, 68.0, 72.4, and 75.11. These peaks can be assigned to CuO.

3.3. Morphology and elements analysis

The morphology of the adsorbent material, which has a heterogeneous composition, is depicted in Fig. 7, showing agglomeration of particles packed together. Due to their small size relative to the surface, these particles exhibit interparticle bonding forces. Fig. 8 shows how the surface became denser and more complex with a relatively uniform distribution of copper oxide nanoparticles in the structure. Fig. 9 shows the main peaks of carbon, nitrogen, and oxygen in the material produced from the first development stage (CT-GLA-PD). The presence of copper peaks in the material produced from the second development stage demonstrates the successful bonding of copper nanoparticles (CT-GLA-PD-Cu) as shown in Fig. 10.

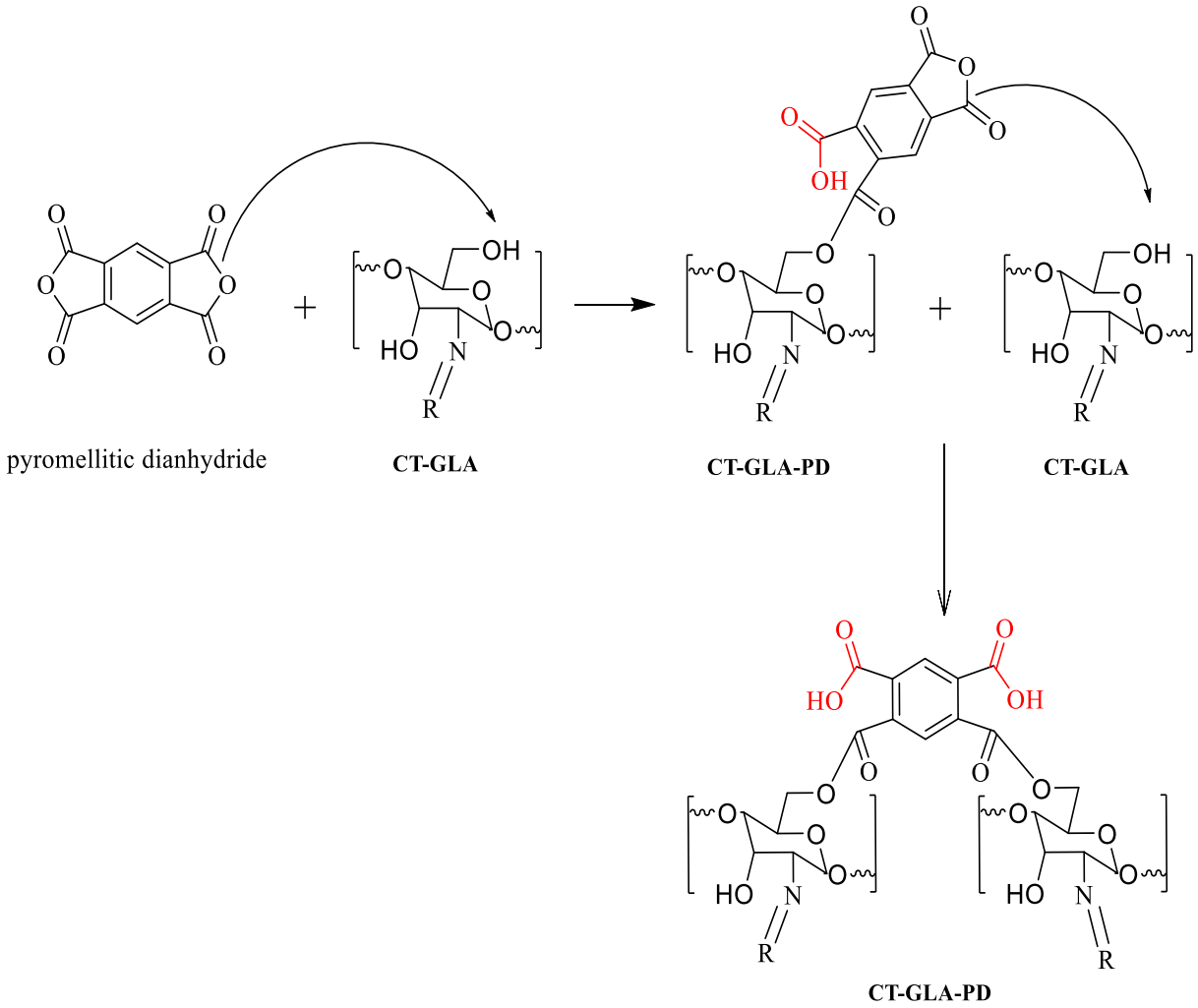

Fig. 5. Schematic diagram presenting the reaction mechanism of chitosan-based glutaraldehyde and pyromellitic dianhydride

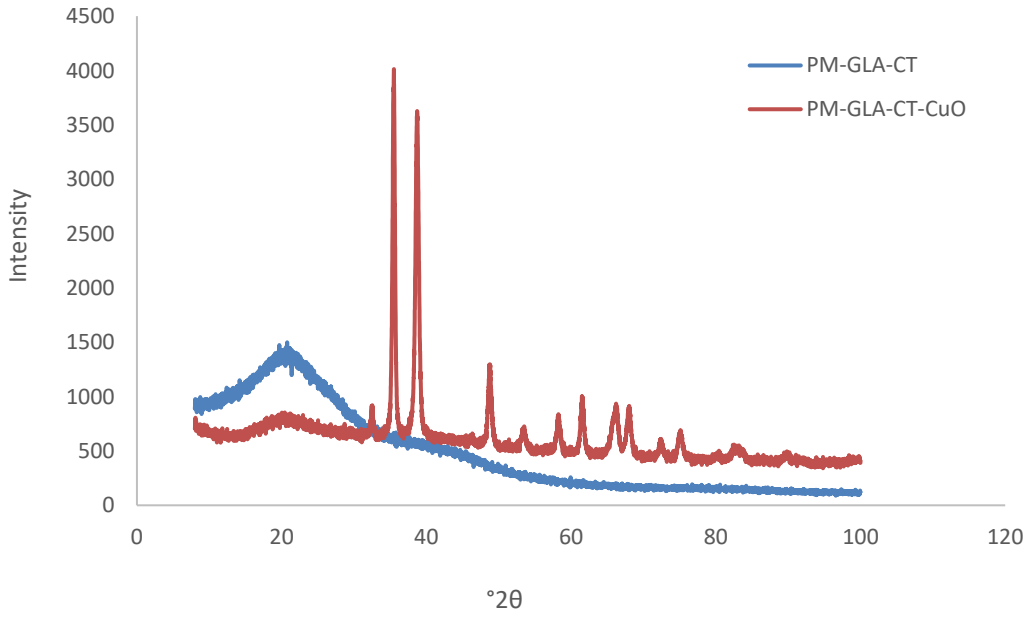

Fig. 6. X-ray diffraction spectra (XRD) of chitosan-glutaraldehyde-pyromellitic dianhydride (CT-GLA-PD), chitosan-glutaraldehyde-pyromellitic dianhydride-copper (CT-GLA-PD-Cu)

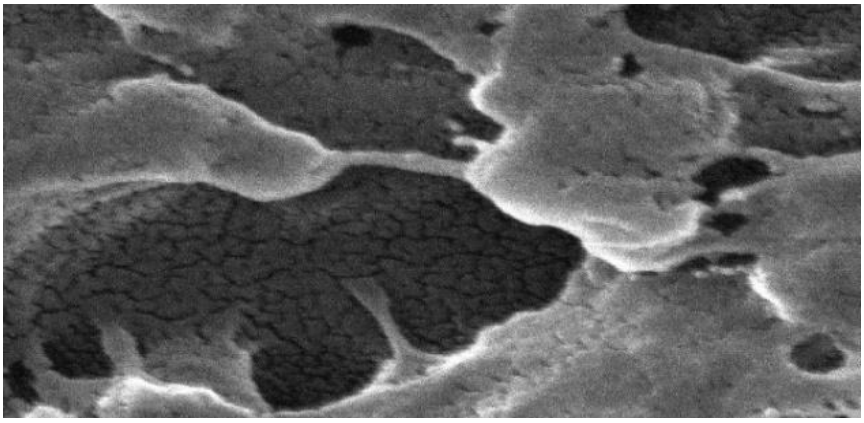

Fig. 7. FESEM of chitosan-based glutaraldehyde and pyromellitic dianhydride (CT-GLA-PD)

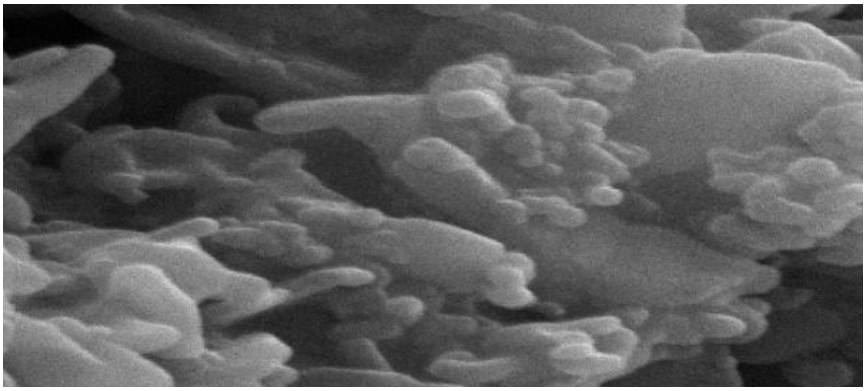

Fig. 8. FESEM of chitosan-based glutaraldehyde, pyromellitic dianhydride, and copper oxide nanoparticles (CT-GLA-PD-Cu)

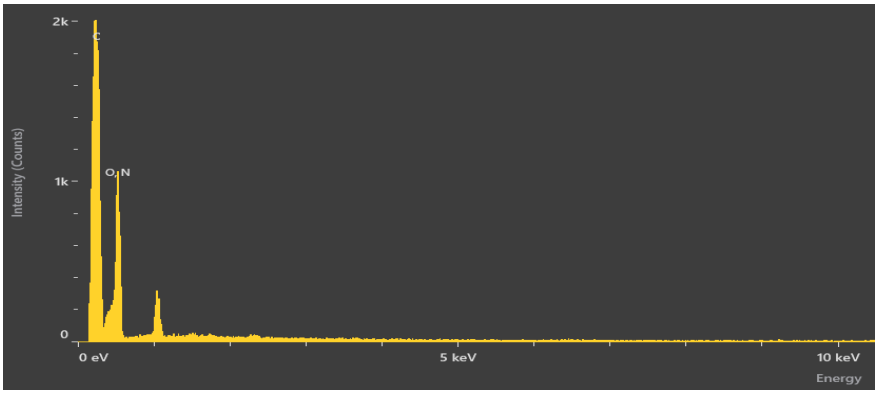

Fig. 9. Energy dispersive X-ray of chitosan-based glutaraldehyde and pyromellitic dianhydride (CT-GLA-PD)

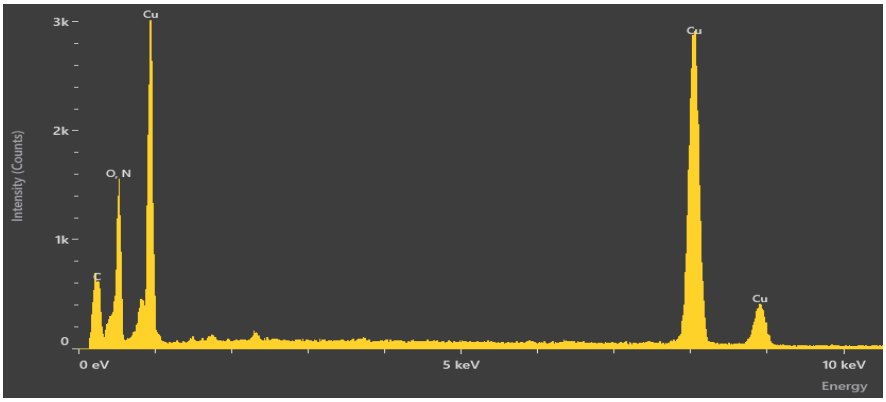

Fig. 10. Energy dispersive X-ray of chitosan-based glutaraldehyde, pyromellitic dianhydride, and copper oxide nanoparticles (CT-GLA-PD-Cu)

3.4. Adsorption performance evaluation

The upgrading of adsorption performance for modified materials produced from the first and second stages was evaluated through removal of lead (II) from contaminated water test as shown in Fig. 11. The results demonstrated a significant improvement in removal efficiency compared to the raw polymeric material. The CT-GLA-PD achieved significant increase in removal efficiency due to chemical modifications, such as crosslinking achieved through glutaraldehyde and the compensation of functional groups from the heterogeneous organic rings. Nanoparticles played an important role in improving the surface structure of the adsorbent and the homogeneous distribution of functional groups, resulting in an additional improvement in removal efficiency. These results are consistent with previous studies, for example, Kandile et al. [13] and Fouda et al. [25]. They demonstrated that chemical modification of polymers with organic compounds with heterogeneous organic rings has a positive effect on removal efficiency. In this study, the effect of heterocyclic organic compounds in improving removal efficiency was confirmed, and the incorporation of nanoparticles into the modified chitosan significantly enhanced its adsorption capacity.

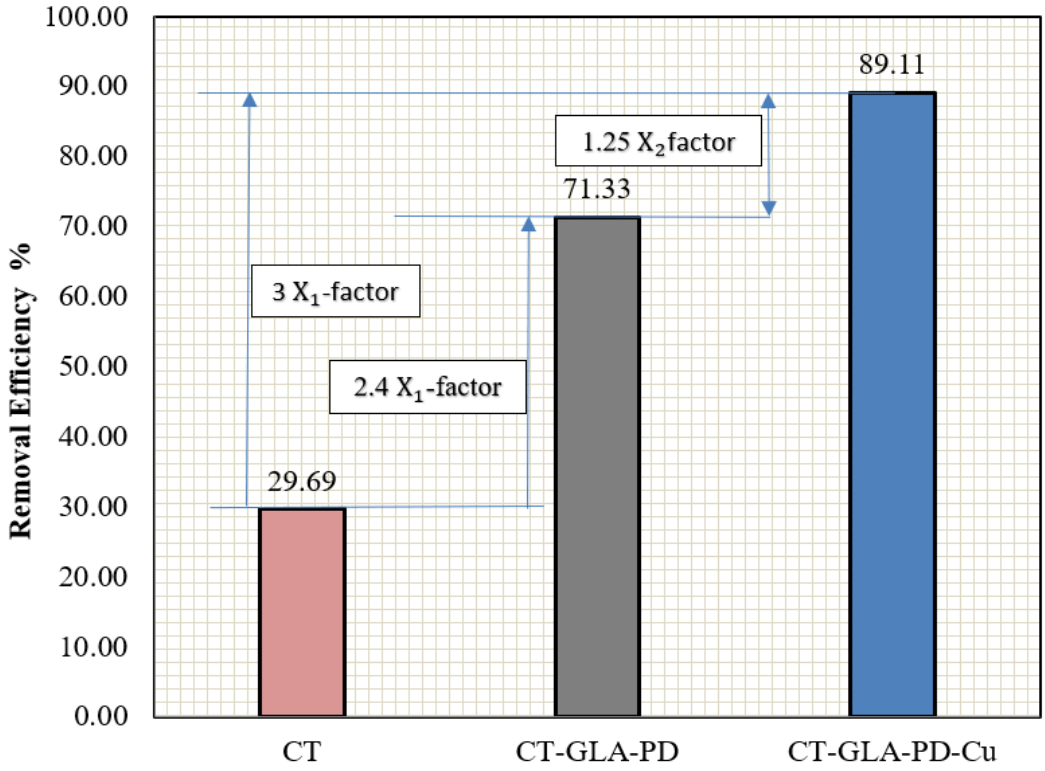

Fig. 11. Removal efficiency of the lead II using nanocomposite during the modification stages (X_1 according to CT, and X_2 according to CT-GLA-PD)

3.5. FTIR after adsorption process

After this stage, the adsorbent samples were tested for their ability to remove lead ions from contaminated water, and an analysis of the behavior was conducted using FTIR. Fig. 12 shows the FTIR spectra before and after Pb (II) adsorption. The broad peak at 3446 cm^{-1} corresponds to O-H stretching vibrations, representing both free hydroxyl groups and bound OH bands of carboxyl groups, which occur across a wide frequency range. The peaks at 2937 and 2877 cm^{-1} correspond to (C-H) Alpha, and the peak at 3100 cm^{-1} relates to (-C-H) Aromatic [26]. The peak at 1718 cm^{-1} is associated with (C=O) in carboxylic groups, while peaks at 1654 and 1693 cm^{-1} relate to (C=O) in amides. The strong band at 1593 cm^{-1} represents (C=C) stretching in benzene rings. Peaks between 1111 and 1055 cm^{-1} may be caused by C-OH stretching vibrations of carboxylic acids. The absorbance peaks shifted between the spectra before and after Pb (II) sorption, indicating interaction between Pb (II) and the functional groups of the adsorbent.

The asymmetrical stretching vibration at 3417 cm^{-1} was notably altered after Pb (II) sorption, suggesting a chemical interaction between the metal ions and hydroxyl groups on the sorbent surface. A slight shift was observed in the C-O band from 1100 cm^{-1} to 1033 cm^{-1}. The peak at 1707 cm^{-1} 1635 cm^{-1} compared with 1718-1654 cm^{-1} indicating the involvement of OH groups in binding Pb (II). FTIR of CT-GLA-PD with CuO before and after adsorption of lead ion under acidic conditions is shown in Fig. 13. New bands appeared around 600 and 800 cm^{-1}: the band at 600 cm^{-1} is attributed to the asymmetric stretching vibration of lead-OH, and the band at 800 cm^{-1} is linked to Pb-O vibrations of the inner sphere Cu-Pb complex.

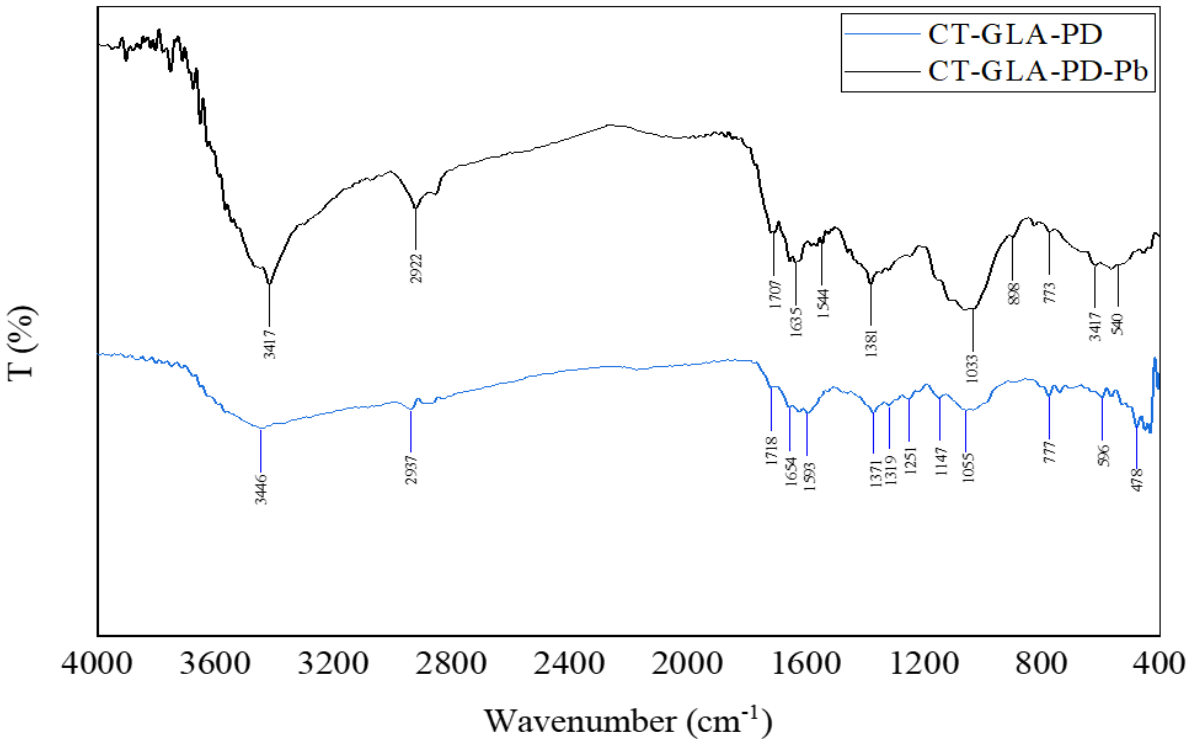

Fig. 12. FITR spectra of chitosan-glutaraldehyde-pyromellitic dianhydride (CT-GLA-PD) before and after adsorption

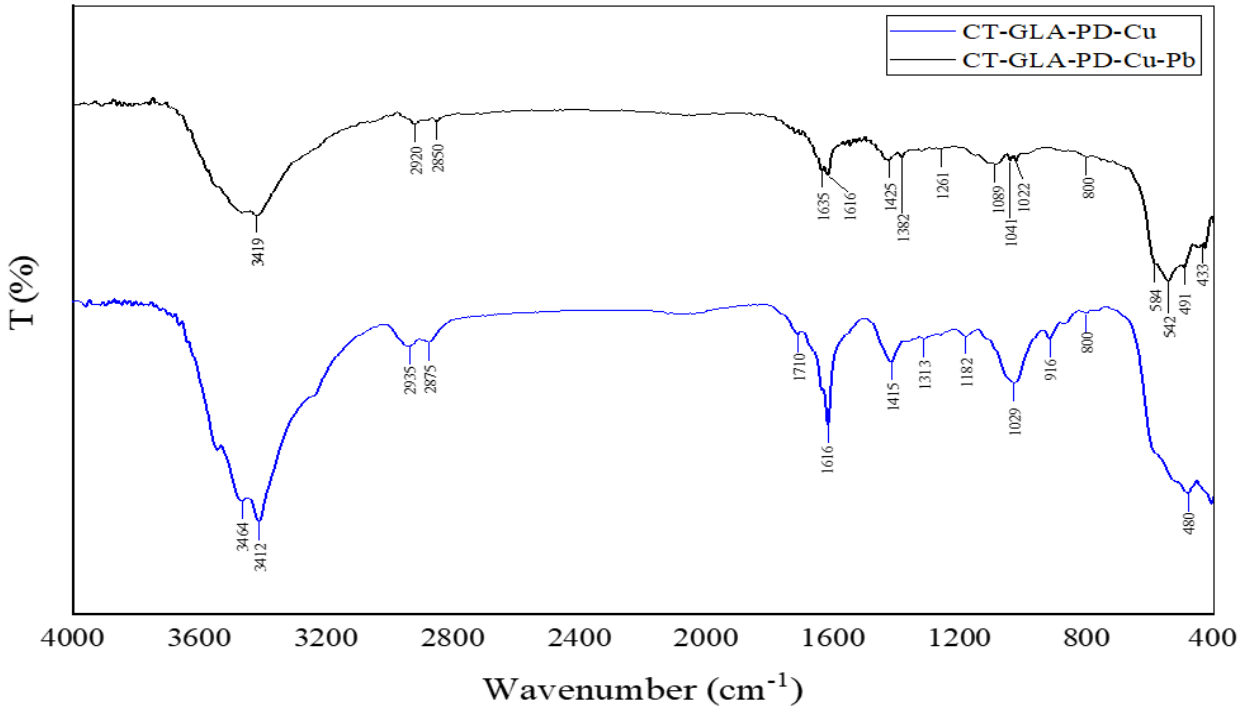

Fig. 13. FITR spectra of chitosan-glutaraldehyde-pyromellitic dianhydride-copper (CT-GLA-PD-Cu) before and after adsorption

4- Conclusion

A new adsorbent material based on an environmentally friendly, biodegradable, and non-toxic organic polymer was successfully prepared. The material underwent a series of advanced analyses: XRD, EDX, FE-SEM, and FTIR to determine the crystalline and surface properties of the two samples, as well as their functional groups in the chemical structure. The results revealed that the predominant surface characteristic was a heterogeneous structure with clusters of nanoparticles, confirming the samples' good crystallinity. Consequently, the appearance of functional groups during the first and second stages contributed to a significant improvement in the removal rate of lead from contaminated water.

Acknowledgement

The authors would like to thank the College of Engineering-Department of Chemical Engineering and College of Science for Women-Department of Chemistry at the University of Baghdad for their support in completing this study, providing all available resources.

References

[1] F. Wu, B. C. Campbell, P. Greenfield, G. C. Hose, D. J. Midgley and S. C. George "There and back again: Genomic insights into microbial life in a recirculating petroleum refinery wastewater biotreatment system," *Microbiological Research,* vol. 301, p. 128299, 2025. https://doi.org/10.1016/j.micres.2025.128299

[2] M. J. Stapleton and F. I. Hai, "Microplastics as an emerging contaminant of concern to our environment: a brief overview of the sources and implications," *Bioengineered,* vol. 14, p. 2244754, 2023. https://doi.org/10.1080/21655979.2023.2244754

[3] M. S. H. Qaiser, I. Ahmad, S. R. Ahmad, M. Afzal and A. Qayyum, "Assessing Heavy Metal Contamination in Oil and Gas Well Drilling Waste and Soil in Pakistan," *Polish Journal of Environmental Studies,* vol. 28, pp. 785-793, 2019. https://doi.org/10.15244/pjoes/85301

[4] A. W. A. Sultan, A. A. Alhello, M. A. Aribi and H. T. Al-Saad, "Assessment of hydrocarbons and trace metals pollution in water and sediments of the Fertilizer Plant wastes in Khor Al-Zubair, Iraq," *Mesopotamian Journal of Marine Sciences,* vol. 28, pp. 17-28, 2013. https://doi.org/10.58629/mjms.v28i1.152

[5] E. E. Bestawy, M. A. Rass and M. A. Abdel-Kawi, "Removal of Lead and Oil Hydrocarbon from Oil Refining Contaminated Wastewater Using Pseudomonas spp," *Journal of Natural Sciences Research,* vol. 3, pp. 112-124, 2013.

[6] A. Rivas-Sanchez, A. Cruz-Cruz, G. Gallareta-Olivares, R. B. González-González, R. Parra-Saldívar and H. M. N. Iqbal, "Carbon-based nanocomposite materials with multifunctional attributes for environmental remediation of emerging pollutants," *Chemosphere,* vol. 303, p. 135054, 2022. https://doi.org/10.1016/j.chemosphere.2022.135054

[7] Z. Xu, S. Gu, D. Rana, T. Matsuura and C. Q. Lan, "Chemical precipitation enabled UF and MF filtration for lead removal," *Journal of Water Process Engineering,* vol. 41, p. 101987, 2021. https://doi.org/10.1016/j.jwpe.2021.101987

[8] A. Lalmi, K.-E. Bouhidel, B. Sahraoui and C. e. H. Anfif, "Removal of lead from polluted waters using ion exchange resin with Ca (NO3)2 for elution," *Hydrometallurgy,* vol. 178, pp. 287-293, 2018. https://doi.org/10.1016/j.hydromet.2018.05.009

[9] A. Khiter, O. Arous, N. Nasrallah, N. Abdellaoui, D. Meziani, M. Trari, P. Loulergue and A. Szymczyk, "Removal of lead by membrane photo-electrolysis," *Separation and Purification Technology,* vol. 378, p. 134565, 2025. https://doi.org/10.1016/j.seppur.2025.134565

[10] A. M. Badran, U. Utra, N. S. Yussof and M. J. K. Bashir, "Advancements in Adsorption Techniques for Sustainable Water Purification: A Focus on Lead Removal," *Separations.* vol. 10, pp. 1-26, 2023. https://doi.org/10.3390/separations10110565

[11] A. M. Ridha, "Removal of Lead (II) from Aqueous Solution Using Chitosan Impregnated Granular Activated Carbon," *Journal of Engineering,* vol. 23, pp. 46-60, 2017. https://doi.org/10.31026/j.eng.2017.03.04

[12] S. Shang, X. Li, H. Wang, Y. Zhou, K. Pang, P. Li, X. Liu, M. Zhang, W. Li, Q. Li and X. Chen, "Targeted therapy of kidney disease with nanoparticle drug delivery materials," *Bioactive Materials,* vol. 37, pp. 206-221, 2024. https://doi.org/10.1016/j.bioactmat.2024.03.014

[13] N. G. Kandile, H. M. Mohamed and M. I. Mohamed, "New heterocycle modified chitosan adsorbent for metal ions (II) removal from aqueous systems," *International Journal of Biological Macromolecules,* vol. 72, pp. 110-116, 2015. https://doi.org/10.1016/j.ijbiomac.2014.07.042

[14] A. A. Fadhil and M. E. Ahmed, "Characterization of copper based chitosan nanoparticles synthesis by chemical method: Approach cytotoxic effects on MCF-7 cells," *Iraqi Journal of Chemical and Petroleum Engineering,* vol. 26, pp. 39-50, 2025. https://doi.org/10.31699/IJCPE.2025.3.5

[15] S. Jian, J. Liu, J. Wu, W. Yang, L. Ran, J. Hu, G. Duan, H. Yang, J. Ma and S. Jiang, "Glutaraldehyde-crosslinked chitosan microspheres encapsulating La (OH)3 by electrospraying for efficient remediation of fluoride ions," *Chemical Engineering Journal,* vol. 512, p. 162470, 2025. https://doi.org/10.1016/j.cej.2025.162470

[16] B. A. Ávila Camacho, M. A. Rojas Pabón, N. A. Rangel Vázquez, E. A. Márquez Brazón, H. E. Reynel Ávila, D. I. Mendoza Castillo and Y. A. Huerta, "Adsorption of Pharmaceutical Compounds from Water on Chitosan/Glutaraldehyde Hydrogels: Theoretical and Experimental Analysis," *Polysaccharides* vol. 6, pp. 1-17, 2025 https://doi.org/10.3390/polysaccharides6040090

[17] M. Tavassoli, R. Abedi-Firoozjah, B. Bahramian, M. Hashemi, S. M. A. Noori, N. Oladzadabbasabadi, A. Nagdalian and S. M. Jafari, "Glutaraldehyde cross-linking for improving the techno-functional properties of biopolymeric food packaging films; a comprehensive review," *Food Chemistry,* vol. 478, p. 143740, 2025. https://doi.org/10.1016/j.foodchem.2025.143740

[18] Z. S. Abdulsada*, S. S. Hassan and S. H. Awad*, "Removal of Some Heavy Metals from Polluted Water Using New Schiff Base for Polyacrylamide with Zeolite Nanocomposites," *Baghdad Science Journal,* vol. 21, pp. 2838-2852, 2024. https://doi.org/10.21123/bsj.2024.8591

[19] M. A. Munusamy, M. Bharathi, A. H. Hirad, A. A. Alarfaj, S. H. Hussein-Al-Ali, S. Sampath and A. Kudumba, "An Escin-loaded Glutaraldehyde-Albumin nanoparticle system for enhancing anticancer activity on lung cancer A549 cells," *Results in Chemistry,* vol. 13, p. 102021, 2025. https://doi.org/10.1016/j.rechem.2025.102021

[20] Y. Wang, X. Zhang, N. Han, Y. Wu and D. Wei, "Oriented covalent immobilization of recombinant protein A on the glutaraldehyde activated agarose support," *International Journal of Biological Macromolecules,* vol. 120, pp. 100-108, 2018. https://doi.org/10.1016/j.ijbiomac.2018.08.074

[21] X. Wei, S. Chen, J. Rong, Z. Sui, S. Wang, Y. Lin, J. Xiao and D. Huang, "Improving the Ca(II) adsorption of chitosan via physical and chemical modifications and charactering the structures of the calcified complexes," *Polymer Testing*, vol. 98, p. 107192, 2021. https://doi.org/10.1016/j.polymertesting.2021.107192

[22] A. OU and I. BO, "Chitosan Hydrogels and their Glutaraldehyde-Crosslinked Counterparts as Potential Drug Release and Tissue Engineering Systems - Synthesis, Characterization, Swelling Kinetics and Mechanism," *Journal of Physical Chemistry and Biophysics,* vol. 7, pp. 1-7, 2017. https://doi.org/10.4172/2161-0398.1000256

[23] I. Kavianinia, P. G. Plieger, N. J. Cave, G. Gopakumar, M. Dunowska, N. G. Kandile and D. R. K. Harding, "Design and evaluation of a novel chitosan-based system for colon-specific drug delivery" *International Journal of Biological Macromolecules,* vol. 85**,** pp. 539-546, 2016. https://doi.org/10.1016/j.ijbiomac.2016.01.003

[24] M. S. Usman, N. A. Ibrahim, K. Shameli, N. Zainuddin and W. M. Yunus in Copper Nanoparticles Mediated by Chitosan: Synthesis and Characterization via Chemical Methods, *Molecules,* vol. 17, pp. 14928-14936, 2012. https://doi.org/10.3390/molecules171214928

[25] S. R. Fouda, A. Abuessawy, A. A. H. Abdel-Rahman, H. S.El-Hema, M. N. Eisa and M. A. Hawata, "New functionalized magnetite chitosan–heterocyclic nanocomposites excelling in Cd2+ removal from aqueous solution with biological activity," *Applied Water Science,* vol. 15, p. 31, 2025. https://doi.org/10.1007/s13201-024-02353-6

[26] S. M. Ali and S. A. A. Sahib, "Preparing a Compound of New Nanoparticles of Lactam, PE to Improve Their Specifications," *Baghdad Science Journal*, vol. 21, pp. 1332-1331 2024. https://doi.org/10.21123/bsj.2023.8537

الكيتوزان المتشابك مع الغلوتارالدهيد والمعزز بجسيمات نانوية لمعالجة مياه الصرف الصحي: تعديل التركيب الكيميائي

اروى رعد ابراهيم [١]، بسمة عباس عبد المجيد [١،*]، سناء عبد الصاحب [٢]

١ قسم الهندسة الكيمياوية، كلية الهندسة، جامعة بغداد، العراق
٢ قسم علوم كيمياء، كلية العلوم للبنات، جامعة بغداد، العراق

الخلاصة

يُعد تلوث الرصاص الثنائي الناتج عن الصناعات المختلفة مشكلة بيئية خطيرة تتطلب اهتمامًا عاجلاً نظرًا لاستقراره وعدم قابليته للتحلل البيولوجي. يتناول البحث الحالي تطوير البنية الكيميائية لبوليمر طبيعي لإنتاج مركب نانوي ماز لإزالة الرصاص. اعتمد هذا التطوير على المجموعات الوظيفية المتاحة (مجموعات الأمينو $-NH_2$ والهيدروكسيل $-OH$) في البوليمرات الحيوية لإنشاء مادة مازة من خلال خطوتين. تمثلت الخطوة الأولى في الارتباط الكيميائي مع الغلوتارالدهيد كعامل تشابك(CT–GLA)، باستخدام تقنية التشابك المستحلب، متبوعًا برابط آخر مع مركب عضوي غير متجانس لتوفير مجموعات وظيفية إضافية (CT–GLA–PD). تضمنت الخطوة الثانية دعم المركب بجسيمات نانوية من أكسيد النحاس (CT–GLA–PD–Cu) لتحسين البنية الكيميائية للمادة المازة. تم تنفيذ البنية الكيميائية للمواد المحضرة عن طريق تشتت البارافين متبوعًا بدعم الجسيمات النانوية لتفسير المجموعات الوظيفية التي اختفت وتشكلت أثناء مراحل التحضير. تم إجراء توصيف السطح والتركيب الكيميائي للمادة المازة الناتجة عن المرحلتين باستخدام تقنيات وصفية متقدمة مثل مطيافية الأشعة تحت الحمراء بتحويل فوريه، وحيود الأشعة السينية، ومجهر المسح الإلكتروني ذي الانبعاث الميداني، والأشعة السينية المشتتة للطاقة. ووفقًا للبيانات التجريبية، أظهر التعديل الكيميائي تحسنًا ملحوظًا في خصائص الشكل وعناصر التركيب، مما أثر إيجابًا على كفاءة الإزالة. انعكس هذا التطور البنيوي على كفاءة إزالة الرصاص مقارنةً بالمادة المازة الخام. وأظهرت النتائج أن المادة المازة المُنتجة من المرحلة الأولى حققت كفاءة مقبولة في إزالة الرصاص. وتضاعفت هذه الكفاءة بعد استخدام الجسيمات النانوية كمادة داعمة في المرحلة الثانية.

الكلمات الدالة: الامتزاز، الكيتوزان، أكسيد النحاس، المركب، المستحلب، الغلوتارالدهيد.